



An Automated Liver Vasculature Segmentation from CT Scans for Hepatic Surgical Planning

Omar Ibrahim Alirr^{1,2*}, Ashrani Aizzuddin Abd Rahni²

¹College of Engineering and Technology,
American University of the Middle East, KUWAIT

²Department of Electrical, Electronic and Systems Engineering, Faculty of Engineering and Built Environment
Universiti Kebangsaan Malaysia, 43600 UKM Bangi, Selangor, MALAYSIA

*Corresponding Author

DOI: <https://doi.org/10.30880/ijie.2021.13.01.017>

Received 25 May 2020; Accepted 1 November 2020; Available online 30 January 2021

Abstract: Liver vasculature segmentation is a crucial step for liver surgical planning. Segmentation of liver vasculature is an important part of the 3D visualisation of the liver anatomy. The spatial relationship between vessels and other liver structures, like tumors and liver anatomic segments, helps in reducing the surgical treatment risks. However, liver vessels segmentation is a challenging task, that is due to low contrast with neighboring parenchyma, the complex anatomy, the very thin branches and very small vessels. This paper introduces a fully automated framework consist of four steps to segment the vessels inside the liver organ. Firstly, in the preprocessing step, a combination of two filtering techniques are used to extract and enhance vessels inside the liver region, first the vesselness filter is used to extract the vessels structure, and then the anisotropic coherence enhancing diffusion (CED) filter is used to enhance the intensity within the tubular vessels structure. This step is followed by a smart multiple thresholding to extract the initial vasculature segmentation. The liver vasculature structures, including hepatic veins connected to the inferior vena cava and the portal veins, are extracted. Finally, the inferior vena cava is segmented and excluded from the vessels segmentation, as it is not considered as part of the liver vasculature structure. The liver vessel segmentation method is validated on the publically available 3DIRCAD datasets. Dice coefficient (DSC) is used to evaluate the method, the average DSC score achieved a score 68.5%. The proposed approach succeeded to segment liver vasculature from the liver envelope accurately, which makes it as potential tool for clinical preoperative planning.

Keywords: Vasculature segmentation, surgical planning, abdominal CT, vesselness, CED

1. Introduction

The segmentation of hepatic vasculature from CT scans is a critical step for hepatic diagnosis, it plays a crucial role and considered as prerequisite step in many clinical applications like liver surgical resections and living donor liver transplantations (LDLT). Surgical resection is widely accepted as treatment to handle metastases appear inside the liver, since the liver has the property of regeneration. Liver vasculature segmentation is an important step to define the segmental anatomy for liver resection planning. However, the resectability depends on tumors size, location, and their relationship with liver vasculature. Tumors located near the vessels may be unresectable, it must be guaranteed that the tumor-free liver tissues remain supplied by the vascular system. This requires an accurate knowledge about the structure

of the hepatic vasculature and the tumors ¹ inside the liver organ. In addition, the LDLT treatments needs a precise analysis of the liver vasculature anatomy to guarantee the donor safety and the functionality of the liver in the patient ².

In general, an accurate segmentation of the liver vasculature can be accomplished manually using an expert radiologist by delineating vessels in each slice of the CT scan. However, this work is tedious, time-consuming and biased to the expert experience. Therefore, the automatic vessels segmentation attracts high research attention. However, automatically differentiating the hepatic vessels from the rest of the liver tissue is not a straightforward process and faces many challenges. These challenges include complexity of the vascular anatomy, the anatomical variability from patient to another, low contrast of the vessels boundaries with the surrounding liver parenchyma, the existence of lesions and the non-uniform intensity values due to contrast injection ³.

In this paper, the main aim is to segment the hepatic vessels in liver envelope. For that, a fully automatic segmentation method is developed. The proposed method aims to extract the two major venous vessels inside the liver organ; the hepatic veins and the portal veins. The paper starts by presenting the main framework of the proposed method. The method starts by a preprocessing step to enhance the appearance of the hepatic vessels in the CT scans. Two different vessels enhancement techniques are used; vesselness filtering and coherence enhancing diffusion filtering. Second, an adaptive thresholding is applied to extract the initial segmentation of the hepatic vessels. Third step is the inferior vena cava (IVC) removal, which is removed from the segmented liver vasculature as it is not considered as part of it ⁴. Finally, the connected component analysis is applied to exclude non-vessels objects from the segmented hepatic vessels. The method is fully automatic and does not require any user interaction.

Nomenclature:

CED	Coherence Enhancing Diffusion
CT	Computed Tomography
DSC	Dice coefficient
EED	Edge Enhancing Diffusion
HDCS	Hybrid Diffusion with Continuous Switch
IVC	Inferior Vena Cava
LDLT	Living Donor Liver Transplantation
VED	Vesselness-Enhancing Diffusion

1.1 Related Works

Liver vasculature segmentation step is as essential step in computer aided systems for liver surgical treatments ⁵. Extracting vessels information from 3D images has been investigated with high interest because of its high importance in variety of medical applications. Many segmentation techniques have been proposed for vessel segmentation. However, general vessels segmentation cannot be used for hepatic vessels segmentation, due its high structural variations, branching complexity and small ending vessel size. For liver vasculature segmentation, a few methods have been published ^{6-14 15}.

In skeleton-based approaches, the aim is to directly find the blood vessel centerlines and then connect the centerlines to form the vessel tree; however, most of these techniques are interactive, as it needs a large amount of user intervention. The user must mark the starting and ending points for each vessel branch, which makes it not feasible to be used to segment complex vessel trees ¹⁶. Shen et al. proposed an interactive skeleton based method, it starts by thresholding the vessels to construct the binary image of vessel structure. Then, extract the skeletonization by analyzing the local maxima voxels in the distance map of the vessel structure. To avoid skeleton redundancy, the selection of connectedness voxel is carried by selecting the first three largest voxels above a threshold in the distance map as candidates for skeleton. However, the method still suffer from skeleton redundancy and disconnection ¹⁷.

Soler et al. proposed a method for liver vasculature segmentation, the method started by applying anisotropic diffusion filtering to enhance intensities and preserve the vessels structures. They used a thresholding technique to cluster the liver envelope into three classes, represent the tumors, parenchyma and vessels, the vessels class represent the initial segmentation. Skeletonization is applied to remove false branching based on topological characteristics extracted from the constructed skeleton ¹⁸. Smistad et al. incorporated model based tube detection, parallel centerline extraction algorithm with parallelized region growing method to extract the tubular structure in different body organs including liver from different image modalities ¹⁹.

In region growing approaches, the idea is to group all image voxels that belong to the blood vessels with each other based on a specific criterion such as proximity or intensity similarity ^{2,20,21}. Chi et al. proposed a region growing based method using context-voting approach to segment and separate the vessels in the target CT scans. The technique used the context information of the vessels properties like intensity, saliency, direction and connectivity to group the voxels to the liver vasculature ⁷. However, the author grouped the voxels according to their intensity based on a fixed experimentally measured threshold, which may fail to be generalized to all data sets. Zeng et al. used two different strategies; they used the 3D region growing with Gaussian filtering for thin vessels segmentation and the active contour with k-mean clustering to segment the thick vessel ²².

Beichel et al. proposed segmentation method depend on the portal veins only to segment the liver segments for surgical planning purposes. For this purpose, they used contrast-enhanced data sets with clear portal veins. They used hessian enhancement to enhance the portal veins, followed by segmentation method based on two techniques; thresholding using Otsu algorithm followed by region growing method¹². Luu et al. incorporated region growing method with different filtering techniques, to show the effect of using the different types of multiscale filtering techniques, like Frangi, Erdt and Sato filters, besides diffusion filtering techniques, like Perdon-Malik, Vesselnessenhancing diffusion (VED) and Hybrid Diffusion with Continuous Switch (HDCS) anisotropic diffusion filters, on extracting the liver vessels. In general, they found that the diffusion filtering gave better performance compared to the vesselness filters. The HDCS showed higher performance compared to other filtering techniques²³.

Level-set based deformable active contour methods are considered as one of most popular techniques used in vessels segmentation, since it is easier to be used to extract particular shapes, and able to be adapt wiht complex topologies of objects²⁴. Hong et al. incorporated both the boundary information with region based level sets for vessels segmentation²⁵. Jin et al. used the hessian-based filtering with a level set active contour to segment the liver vasculature, the level set technique is modified to include the Gaussian standard deviation to reduce the effect of Gaussian filter blurring. The authors used synthetic images to evaluate their technique¹⁰.

Pamulapati et al. proposed a graph-cut based technique to segment the liver vessels. The method started by vesselness enhancement step to enhance the vessels in the portal venous phase CT scans. Seeds for the graph cut are generated automatically by thresholding the CT scans, and used to segment the liver vessels⁶. Kaftan et al. proposed an automatic method of two stages method; first stage to segment the big radius vessels using graph cut technique, they incorporated mean Gaussian filter, intensity classification and vesselness steps to automatically define the foreground and background seeds for the graph cut. The second stage is the local tracking of the small size vessels using centrelinebased approach, because it needs highly computational demands, it is applied on the small vessels²⁶. Esneault et al. proposed fully automatic liver vessels segmentation. The method based on graph cut technique constrained by local constructed vessels models. The authors aim to achieve accuracy and robustness by combining the graph cut and the local vessels models¹⁴. Yureidini et al. proposed a semi-automatic model-based method for vessels segmentation, by fitting a cylindrical shape to a volume of points using RANSAC algorithm to find vessels with cylinder shape located perpendicular to the planes. Manual seed selection is required at each branch to track it¹¹.

Zhan et al. proposed a machine learning method based on multilayer neural network to segment the hepatic vasculature. The voxels in the liver region are assigned either as vessel's voxels or as parenchyma voxels to be used in the training step. The method is very sensitive to low contrast between vessels and liver tissue, like it failed to segment portal veins²⁷.

2. The Proposed Method

The general framework is presented by the flowchart shown in figure 1. It consists of four main steps: Preprocessing, initial vasculature segmentation, small objects removal and inferior vena cava removal. The system inputs are the clinical CT scans acquired in the portal venous phase (PVP) and the liver organ envelope²⁸.

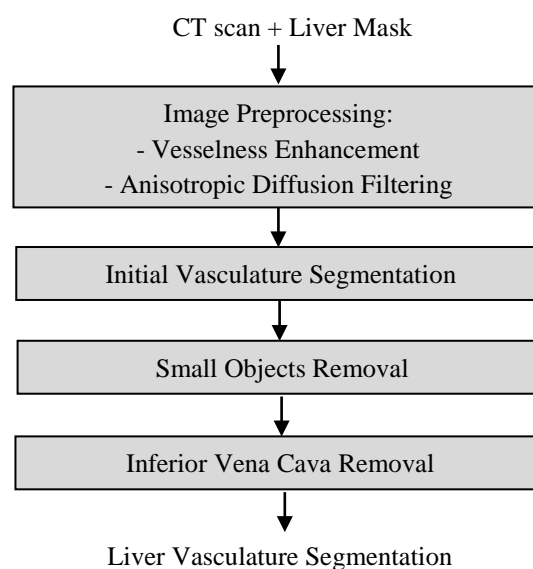


Fig. 1- Flowchart of the liver vasculature segmentation method

2.1 Image Preprocessing

The noise in CT scans has two main sources, patient body motion and noise caused by the CT scanner. CT scans with high resolution, will be subjected more of the CT scanner noise. This noise cannot be overlooked since it has high effect on the vessels structure. Therefore, a pre-processing procedure is developed for vessel enhancement and noise filtering before starting the vessels segmentation.

Vessels enhancement could be accomplished either by noise reduction filters or by vesselness filters. Luu et al. 2015 made a quantitative comparison between the diffusion filters and vesselness filters for liver vessels enhancement. They stated that diffusion filters perform better than vesselness filters for large vessels that have high contrast and clear boundaries. In addition, it works well at vessels bifurcations, compared to vesselness filters, which do not perform well in these cases. On the other hand, Vesselness filters are better to enhance the small low contrast vessels, compared to the diffusion filtering which based on smoothing that may lead the low contrast vessel to disappear. Thus, the vesselness filtering is better for low contrast small vessels, and the diffusion filters are more suitable for high contrast large vessels ²³.

In this paper, a novel approach is proposed by combining vesselness enhancement and diffusion filtering techniques to extract the vessels structure in the target CT scans. The aim is to utilize the benefits of these two techniques and overcome their limitations as explained in ²³. The hessian based Frangi vesselness filter is used to enhance the vessels structure and weakens the non-tubular like structures. Anisotropic coherence enhancing diffusion filtering (CED) is applied on the vesselness-enhanced image. The vesselness filter aims to enhance and extract the tube like structures and the coherence-enhancing filter is used to denoise the errors and enhance the coherence of the regions with similar intensities while preserving the vessels edges.

a. Vesselness Enhancement

The hepatic and the portal veins are enhanced with contrast and has a relatively higher intensity compared to the liver parenchyma in portal venous phase CT scans. However, some data sets come with low contrast to noise ratio. In order to enhance and preserve the vessels structure, the vesselness filters are used. Many types of vesselness enhancement filters have been used, all of it intend to enhance the tube-like structure and suppress other structures. In this work the Hessian-based multi-scale filtering based on the work of Frangi ²⁹ is applied, it aims to differentiate the tubular like structures from blob and plate like structures. The main idea is that the images are convolved with 3D Gaussian filters at multiple scales, and the eigenvalues of the Hessian matrix at each pixel or voxel are analyzed in terms of a response function to determine the shape of the local structures inside the images. For each scale σ , which represent the vessels radius, the discrimination function, i.e. vesselness is measured by the Equation 1.

$$v(\sigma) = \begin{cases} 0 & , \lambda_2 \geq 0, \lambda_3 \geq 0 \\ [1 - e^{(-R_a^2/2\alpha^2)}] e^{(-R_b^2/2\beta^2)} [1 - e^{(-S^2/c)}] & , else \end{cases} \quad (1)$$

Where;

$$R_a = \frac{|\lambda_2|}{|\lambda_3|} \quad R_b = \frac{|\lambda_1|}{\sqrt{|\lambda_2\lambda_3|}}$$

are the parameters that differentiate between the tube-like structure from plate like structures, and from blob like structures, respectively. Where $|\lambda_1| \leq |\lambda_2| \leq |\lambda_3|$ are the eigenvalues of the hessian matrix in 3D dimensions. S, represent the Hessian matrix Frobenius norm, it deal with the difference between vessels and the background. The constants α , β and c are constants which tune the sensitivity of, R_a , R_b and S of the vesselness in Equation (1). In this paper the α and β are set to 0.5, the value of c depend on the gray scale range of the image, and it is proved that the optimal value of it is the half maximum value of the hessian norm ¹⁰.

The Hessian enhancement is applied on the target image at multiple scales on each voxel to calculate the maximum vesselness values. The Hessian enhancement at small scale values (1-3) will improve the contrast of the small vessels, while the enhancement at large scale values (4-8) improves the vessels with large radii ²⁹.

In this paper, the aim is to segment the vessels while separating them at their ends. However, the vessels ends are not clear due to low resolutions and it will be hard to separate them from each other. For this purpose, the vesselness is applied with large-scale values (4-8) in the proposed vessel enhancement step to avoid enhancing those tiny connected ends, and ensuring that the vessels are separated from each other to enable us separating them in the next steps.

b. Anisotropic Coherence Enhancing Diffusion Filtering

The best way to improve the contrast in the target CT scans is by reducing the noise and improving the smoothness in the homogeneous intensity regions. For better vessels extraction from the CT scans, it is required to suppress the artifacts while preserving and enhancing the vessels by maintaining the contrast along their edges. For this purpose, the anisotropic enhancing diffusion filtering proved its superiority above other filtering techniques³⁰. In the linear diffusion filters, to preserve the edge, the scalar diffusion constant should be lowered along the steep edges. However, this will result in noisy edges. In contrast, the anisotropic enhancing diffusion filters used the diffusion tensor to adapt the diffusion along the image structures. This diffusion filtering describes the image structure using a structure tensor, which is based on the use of structure description like structure features or local coherence of structure, as diffusion tensor to steer the diffusion³¹.

Mendrik et al. propose two structure tensors, the coherence enhancing diffusion (CED) and edge enhancing diffusion filters (EED). CED is suitable to filter images and enhance the tube like structures compared to EED³⁰. CED is designed to enhance the tube like structures, it is one dimensional diffusion, so it may have diffusion in one dimension or no diffusion at all. Based on the structure tensor, If the $(\mu_1 > \mu_2 > \mu_3)$ are the eigenvalues in the direction of the eigenvectors V_1, V_2, V_3 of the structure tensor, the CED will have a diffusion in the direction of V_3 . The ratio between the second and third eigenvalues will decide whether the diffusion will be performed or not. For vessels like structures, this ratio is large, while for blob or plate like structure the ratio is small. The eigenvalues of the 3D CED diffusion tensor are defined by Equation 2 as;

$$\lambda_{c1} = \alpha, \lambda_{c2} = \alpha;$$

$$\lambda_{c3} = \begin{cases} 1 & , \mu_2 = 0 \text{ or } \mu_3 = 0 \\ [\alpha + (1 - \alpha)e^{(-\ln(2)\lambda_c^2/k)}] & , \text{else} \end{cases} \quad (2)$$

Where, $k = ((\mu_2/\alpha + \mu_3))^4$, $\alpha = 0.001$ and the λ_c is the CED constant parameter³⁰.

In the preprocessing step, the purpose is to enhance the tube-like structure and suppress the other plate or blob like structures. Vesselness will not guarantee the smoothness diffusion along the vessels boundaries and the coherence of the intensities inside the vessel regions that may result in disconnected vessels. Hence, the coherence enhancing anisotropic diffusion filter CED is incorporated to enhance intensity coherence and smooth the tube-like structures.

Figure 2 shows the data set after the preprocessing step, vesselness followed by CED. Figure 2 (b) shows the vessels brighter than the surrounding liver tissue. It is clear that CED filter succeeded to enhance the diffusion along the regions with intensity coherence that is suitable to close the disconnected parts within the vessels region. In addition, it reduces the diffusivity along the non-coherent structures, which maintain the sharp boundaries of the vessels with the surrounding liver parenchyma. This step considered as an important prerequisite step before applying subsequent vasculature segmentation steps.

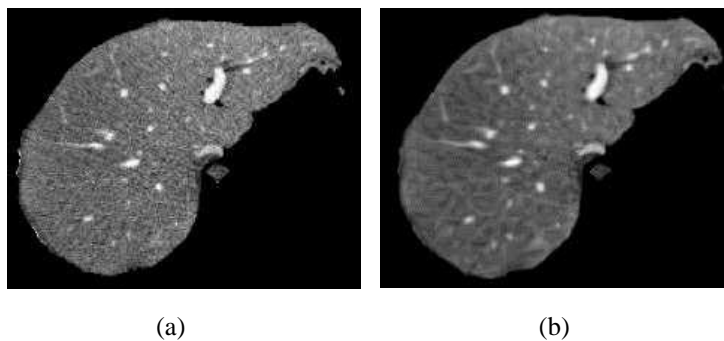


Fig. 2- (a) Original image vs. (b) Enhanced image (Vesselness + CED)

2.2 Initial Vasculature Segmentation

Intensities in the segmented liver region are classified into three groups of intensities. The first is belong to liver parenchyma intensities, which represent the majority of the liver organ and locate in the middle of intensities histogram. The second group represents the low intensities, which include tumors and some parts from the surrounding muscles. The thirds group of intensities belong to the vessel's intensities, which has higher intensity values compared to the liver parenchyma. In the preprocessing step, the aim was to enhance the vessels to make them have high contrast compared to the surrounding liver tissue.

The aim in this step is to extract the vessels intensity cluster. A thresholding method is proposed based on an automatic, fast and robust Otsu technique. In order to facilitate the calculation of the vessel's threshold, the tumor

intensities are excluded. The thresholding method is applied on the intensities that include liver parenchyma and higher intensities. The thresholding aims to find the optimal threshold between the two classes that reduce the within-class variance. However, this threshold will not guarantee the correct discrimination of the vessel's voxels from the liver parenchyma, since the calculated vessel's cluster will include some intensities from the liver tissue that don't belong to the vessels. This is because that the majority of the pixels inside the liver envelop belong to the liver parenchyma, which have low intensity values compared to the vessel's intensities. That would affect the between class's variance computation and pulls the calculated threshold toward the liver intensities.

Therefore, the intended vessels threshold is higher than the first computed threshold value. To solve this problem, some works¹³ proposed to assign a fixed threshold to discriminate the vessels intensities for all data sets. However, this is not correct because each data set has different intensity characteristics that could result in different threshold value.

To handle this problem, a smart adaptive thresholding is proposed to find the correct threshold that segregate the vessels voxels from the liver parenchyma, Fig. 3 explains the idea of the proposed multilevel thresholding. The proposed adaptive thresholding aims to apply the multilevel thresholding on the resulted higher intensity cluster, above the first global threshold (T1). The method aims to narrow to the correct threshold by applying the iterative thresholding increasingly on the higher intensities cluster until finding the best threshold that differentiate only those voxels that belong to the vessels from other liver voxels. The best threshold is the threshold above which the optimal vessel's voxels ratio is found.

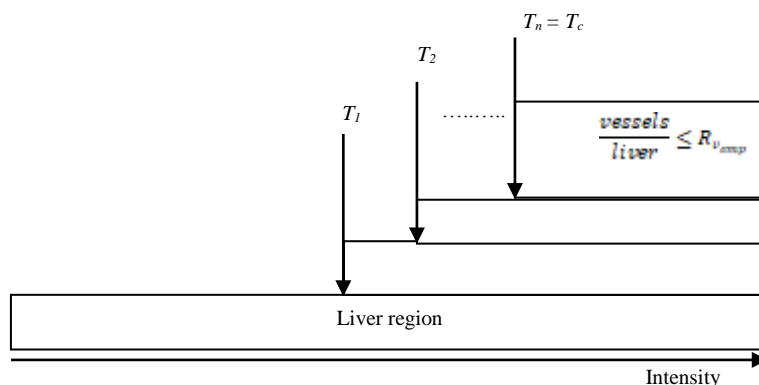


Fig. 3 - Smart multiple thresholding

Anatomically, the vessels structures have small ratio compared to the liver tissue inside the liver organ envelope. This ratio differs for different CT scans based on many reasons, like the amount of contrast inside the vessels or the patient liver anatomical vasculature complexity. In this work and bases on an empirical analysis of many datasets, we found that the empirical value $R_{v_{emp}}$ is about 15%, which is defined as the ratio of vessels intensities with respect to the overall liver intensities is measured. Sure, this ration will not give the exact segregation of vessels from the liver tissue in liver envelope. However, this ratio aims to include the majority of the voxels that belong to the vessels. Depending on this empirical ratio, the correct threshold (T_c) can be estimated using iterative thresholding. The correct threshold (T_c) is defined as the threshold above which the ratio of the vessels is less than or equal the empirical ratio ($R_{v_{emp}}$). Hence, the measured $R_{v_{emp}}$ controls how many thresholding levels (T_1, T_2, \dots) are needed to be applied to find the optimal threshold, where the number of levels depends on the dataset itself. Fig 4 shows the extracted vessels intensities for example dataset, its clear that the main hepatic and portal veins are correctly segmented. However, it can be seen some voxels don't belong to the vasculature are also segmented. These erroneously segmented objects will be refined using a postprocessing step that aims to refine the segmented vasculature and remove non-vessels voxels.

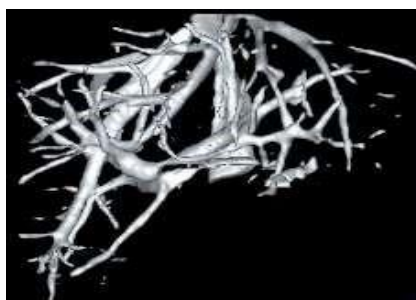


Fig. 4 - Initial vasculature segmentation (3D rendering)

2.3 Small Objects Removal

During the previous steps, some voxels would be enhanced and as a result, it may have intensity values above the vessel computed threshold that make them to be segmented and appear in the output of the thresholding step. In this step, the aim is to refine the output of the previous step, by removing the small objects that do not belong to the vasculature structure. The vessels are connected structures, and those with their voxels are connected in the 3D with six connections are considered. For this purpose, the connected component analysis (CCA) approach is adopted to extract the voxels that belong to the vasculature structure.

The output of the previous step represents the initial liver vasculature segmentation. It includes the hepatic veins, the portal veins and other small objects. The CCA aim to extract the largest two structures from the initial vasculature segmentation. These two structures represent the hepatic veins connected at their roots with the inferior vena cava, and the second large structure is the hepatic portal veins branching from the general portal vein. These two structures represent the initial segmented vasculature.

The step starts by morphological opening trying to separate the connected vessels at their ends. Then the CCA is applied to select the two largest structures from the initial segmented vasculature. Fig. 5 shows the initial segmented vasculature after being refined from non-vessels objects, it can be seen now compared to Fig. 3 that the all segmented voxels are connected and belong to the liver vasculature.

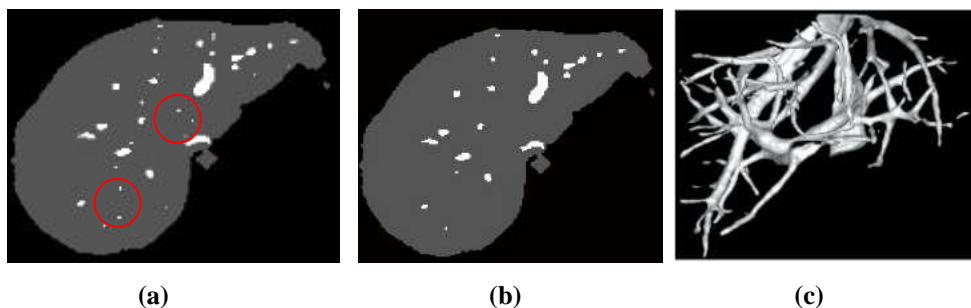


Fig. 5 - (a) 2D Vasculature Segmentation before refinement; (b) 2D after refinement; (c) 3D Rendering of Segmented Vasculature

2.4 Inferior Vena Cava Removal

Inferior vena cava (IVC) is a large vein carrying the deoxygenated blood back to the heart from all human body organs. The hepatic veins roots are connected to IVC to drain the blood from the liver. The inferior vena cava (IVC) is considered as landmark that helps in segmenting the vessels inside the liver. In order not to affect the liver volume calculation, it is required to segment it out.

A procedure to extract the IVC from the segmented vasculature is proposed. The method depends on the vasculature segmentation output from the previous step. The inferior vena cava vein has a straight and tubular shape, based on this anatomical information about the IVC, the proposed method includes two main steps. The first step is to find the starting contour of the IVC by matching an ellipse shape to the IVC part between the liver and heart. Then, the second step is the 2D active contour extension, propagating in each slice sequentially along the IVC structure. The steps are detailed in the next paragraphs. The full details of this step is outlined in a previously published paper ⁴.

Fig. 6 shows the output of IVC extraction process. Fig. 6 (a) shows the extracted IVC, and Fig. 6 (b) shows the final segmented liver vasculature excluding the IVC.

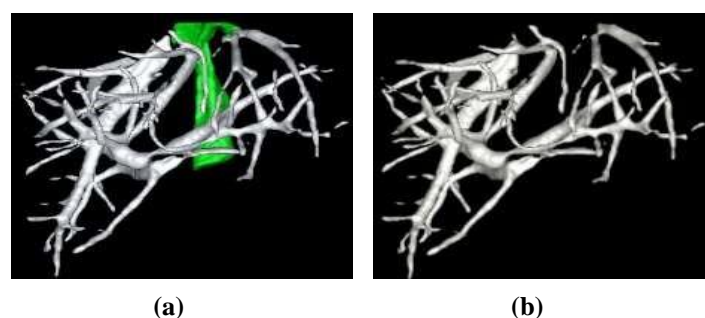


Fig. 6- (a) Extracted IVC in green color; (b) Liver vasculature without IVC

3. Results and Discussion

3.1 Validation Approach

Due to the lack of a reference gold standard datasets for liver vasculature like those for liver organ segmentation, the validation of liver vessels segmentation is very hard to achieve. The ground truth data sets can be obtained using corrosion cast techniques, however these methods require a very expensive device, and it is very tedious. Manual delineation by experts is another way of ground truth extraction, which need a lot of time and mainly biased by the radiologist experience that may lead to inaccurate results³².

In this paper, the vasculature segmentation method is validated against publically available IRCAD data sets, which has ground truth segmentations of the liver vessels. IRCAD dataset¹ has higher variety and complexity of livers and its tumors, IRCAD dataset includes 20 venous phase enhanced CT volumes acquired with different CT scanners. IRCAD data sets are pathological CT cases.

The evaluation of the proposed method outputs is carried in two ways; first qualitatively, by visual inspection of the method results and the comparison with ground truths data. Second, quantitatively, by comparing the method output with their corresponding ground truth using selected evaluation measures.

3.2 Segmentation Results

Fig 7 shows the segmentation of the liver vasculature for three different data sets using the proposed method, where each column represents separate data set example. The first three rows explain the vasculature segmentation in three different axial slices for each data set. The axial slices compared the proposed method results with their corresponding ground truth segmentation. The image axial slices in Fig. 7 demonstrate results of the proposed method by overlaying the segmented vessels mask on the CT scan in the locations where the method succeeded to delineate the liver vasculature. The axial slices explain the main differences between the segmentation method output and the manually delineated vessels (ground-truth), by clarifying the main locations of the under segmentation (false negative) cases (green color) and over segmentation (false positive) cases (blue color). The 3D rendering in the fourth row visualize the vessels segmentation results in the context of the liver organ.

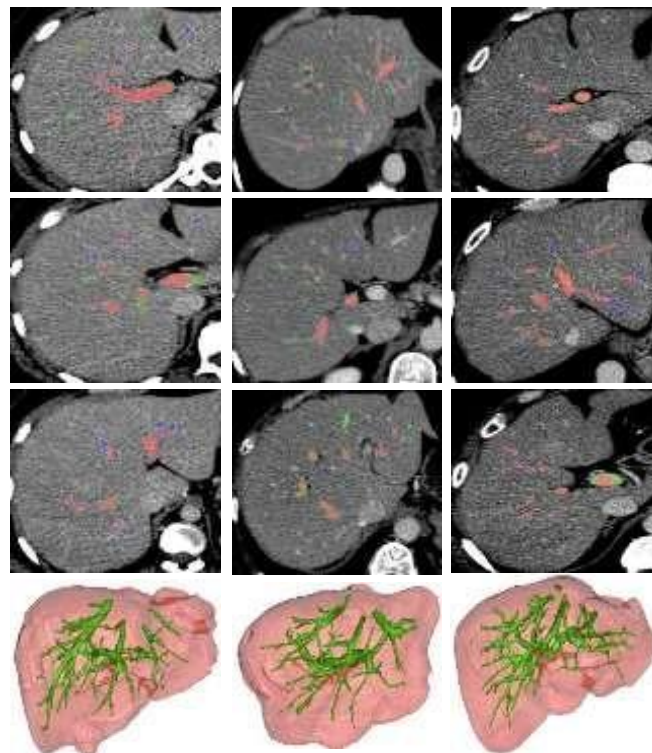


Fig. 7 - Liver vasculature segmentation for different Datasets

¹ available at <http://ircad.fr/research/3d-ircadb-01>

A qualitative evaluation is carried by visual inspection to assess the proposed method results. The qualitative approach aims to demonstrate the main causes of the differences between the ground truth and the segmentation results. Fig. 8 highlights the main scenarios that affect significantly the proposed method segmentation results using visual inspection of one example data set, which can be generalized on other data sets. Fig. 8 (a) shows the 3D rendering of the segmented vessels, Fig. 8 (b) shows the 3D rendering of the corresponding ground truth, and Fig. 8 (c) displays the comparison between the ground truth and the proposed method segmentation for an example data set.

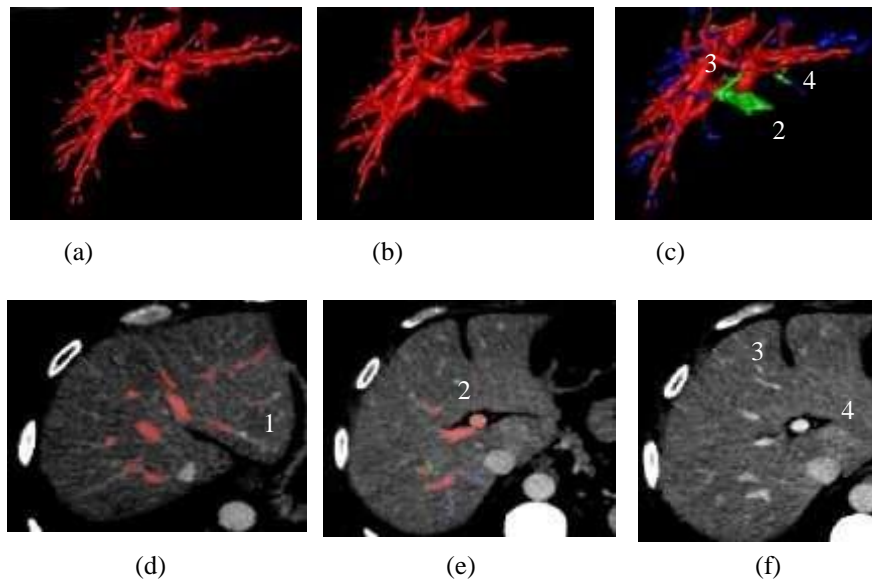


Fig. 8- Visual inspection of the main causes of liver vasculature segmentation Errors

In Fig. 8 (c), the overlap between the ground truth and the segmentation result is in red color. The vessels with blue color represent the over-segmentation (false positive), which is the vessels voxels segmented by the proposed method but not exist in the ground truth. Those voxels that could not be segmented by the proposed method and appear in the ground truth are in green color, it represents the under-segmentation (false negative), of the method.

Initially, it is clear that method succeeded to segment all the major vessels correctly. However, the main differences are in the vessels branches ends and sometimes in vessels surfaces, as will be explained in the next paragraphs. An over-segmentation(false positive) is shown in Fig. 8 (c) marked by number 1, it is not an oversegmented branch, as shown by the slice in Fig. 8 (d), it is a clear branch that is segmented correctly by the proposed method, but it does not appear in the ground truth segmentation.

The under-segmentation case (false negative) marked by the number 2 in Fig. 8 (c) shows an example of the portal vein that is under-segmented in the vessels surface, the Fig. 8 (e) explains that, it shows the segmentation of the portal vein (red color) using the proposed method except the surface at some parts of the vessel.

Number 3 in Fig. 7 (c) marks another under-segmentation case. It represents a correct under-segmented branch, as it appears clear in the slice shown in Fig. 7 (f). This branch has a weak contrast at the bifurcation, which could not be enhanced and extracted using the filtering techniques as proposed in pre-processing step

The last under-segmentation case appears in Fig. 7 (c) is marked by number 4. In this case the contrast of the vessel branch is very low as shown by the slice in Fig. 7 (f), and could not be enhanced or thresholded, which lead to detection failure of the intended branch.

In general, most of the segmentation differences between the segmented vasculature and its corresponding ground truth are at the vessels surfaces and branch tips. The main hepatic veins (right, middle and left) and the portal veins are well segmented. In addition, most of over-segmentation cases occurred at branch tips that are due to the conservative or overlooking by the manual delineations in these places.

3.3 Quantitative Evaluation

It is clear from the visual inspection of the segmentation outputs that the proposed method succeeded to segment the majority of the vasculature tree, especially the major vessels. And the main differences with the ground-truth happen at the tiny ends and major vessels surface. Despite that, for hepatic surgical planning, the aim is to identify the major vessels centerlines that define the liver segments territories and these centerlines are extracted using the core body of the vessels.

To quantitatively assess and evaluate the proposed technique, a group of performance measures are used, namely the accuracy, specificity, sensitivity, Jaccard index and dice coefficient. The voxel segmentation accuracy measures the ratio of the total number of voxels that are correctly classified either as vessels or as liver parenchyma. It is defined by Equation 3 as follow;

$$\text{Accuracy} = \frac{TP + TN}{TP + FN + TN + FP} \tag{3}$$

Where TP (true positive) and TN (true negative) represent the number of voxels correctly classified in the vessels and in the liver parenchyma, respectively. FN (false negative) and FP (false positive) represent the number of voxels that are not correctly classified in the vessels and in the liver parenchyma, respectively.

Other important measures are sensitivity and specificity. Sensitivity shows the correctly segmented voxels from vessels (TP) compared to the ground truth vessels (TP+FN), as shown by Equation 4. The sensitivity measure shows the method ability to segment the vessels voxels correctly from CT scans. On the other hand, the specificity measure shows the ratio of the number of correctly segmented non-vessels voxels using the method over the total number of non-vessels voxels in the liver region of interest. The specificity measure shows how likely the method able to segment the voxels that don't belong to the vessels, the specificity is shown by Equation 5.

$$\text{Sensitivity} = \frac{TP}{TP + FN} \tag{4}$$

$$\text{Specificity} = \frac{TN}{TN + FP} \tag{5}$$

The Jaccard overlap index compares the method results with the manually segmented vessels (ground truth). The Jaccard index, JI, between the segmented vessels and its corresponding ground truth, represent the ratio of the number of correctly segmented vessels voxels over the number of voxels in the union of the ground truth and the segmentation result, as defined by Equation 6.

$$\text{JI} = \frac{TP}{FP + TP + FN} \tag{6}$$

The last measure used is the Dice coefficient (DSC), defined by Equation 7. It is another overlap measure that computes the ratio between the correctly segmented liver voxels (intersection) with respect to the average size between the segmentation output and the ground truth.

$$\text{DSC} = \frac{2 * TP}{FP + 2TP + FN} \tag{7}$$

Table 1 shows the performance results of the vasculature segmentation method. The average segmentation accuracy is 99%. The sensitivity values range from 56% to 80%, with an average value of 65%. The specificity ranges from 98% to 99% with average value 99%. The average segmentation overlap (JI) is 52% with highest value of 66% and minimum value of 47%. For Dice measure (DSC), the average value is 68.5%. The qualitative evaluation carried in the previous section justifies the segmentation method measures values.

Table 1 - Liver vasculature segmentation: quantitative evaluation results

CT scan	Accuracy	Sensitivity	Specificity	JI	DSC
1	0.99	0.59	0.99	0.49	0.66
2	0.99	0.69	0.99	0.54	0.70
3	0.99	0.80	0.99	0.66	0.80
4	0.99	0.58	0.99	0.47	0.64
5	0.99	0.64	0.99	0.59	0.74
6	0.99	0.58	0.98	0.53	0.69
7	0.99	0.74	0.99	0.46	0.63
8	0.99	0.61	0.99	0.49	0.66
9	0.99	0.56	0.98	0.49	0.66
10	0.99	0.68	0.99	0.50	0.67
Average	0.99	0.65	0.99	0.52	0.685

Quantitative comparisons with other segmentation techniques in the literature^{6-10,13,26,27,33}, are hardly feasible to be held for many reasons. First, in liver vasculature segmentation subject, these techniques are few, some authors used their own clinical data sets, and some of them used synthetic data sets and others validated their work on images with constructed shapes (phantoms) similar to vessels⁸. Second, other works implementations are not publicly available. Besides that, most of works proposed to segment the liver vasculature adopted the visual inspection to assess the goodness of their segmentations. Other work proposed region growing based method which is applied on a selected group of datasets from IRCAD, the authors didn't show a full evaluation procedure of their method, and used a few performance measures that don't reflect the segmentation output accuracy, like dice or Jaccard metrics. Rui et al. propose a similar approach to the proposed method; however they used an improved fuzzy connectedness method which is initialized automatically using otsu thresholding³⁴.

Few of these works^{7,8,27,33} presented a detailed evaluation of the method accuracy and errors as presented in this paper. Table 2 presents the proposed method evaluation results along with other methods that have detailed evaluation. The Table does not present a comparative evaluation between the proposed method and the other methods due to the challenges mentioned previously.

Table 2 - The proposed method listed with other previous techniques

Method	Interaction	Sensitivity	Specificity	Accuracy	JI	DSC
Conversano et al. ⁸	Auto	0.723	0.989	0.973	NA	0.949
Zhan et al. ²⁷	Semi	0.742	0.993	0.981	NA	NA
Smistad et al. ¹⁹	Semi	0.571	0.990	0.970	NA	NA
Zhang et al. ³⁵	Auto	0.785	0.98	0.981	NA	NA
Rui et al. ³⁴	Auto	0.737	0.974	0.96	NA	0.673
Chi et al. ⁷	Semi	0.70	0.99	0.98	0.55	0.70
Proposed Method	Auto	0.65	0.99	0.99	0.52	0.685

4. Conclusion

The paper presented a fully automatic method of liver vasculature segmentation from portal venous phase contrast enhanced CT scans. The method demonstrated the effectiveness in segmenting the hepatic and portal veins correctly from all data sets. The framework start by vessels extraction and enhancement filtering, followed by smart multiple thresholding, and end by extracting the vasculature. The proposed method demonstrated the effectiveness in segmenting the hepatic vasculature correctly from all data sets. The errors appear in the results is sufficiently low and mainly on the vessels surface and branches tips, which don not have an effect on making a preoperative treatment planning. The method performs automatically without the need of user interaction. The quantitative and qualitative evaluations of the proposed method promote its ability as clinical tool for preoperative planning in hepatic treatments.

Acknowledgement

This research is supported by the Malaysian Ministry of Higher Education and Universiti Kebangsaan Malaysia under grant no. GUP-2014-066.

References

- [1] Alirr, O. I.; Rahni, A. A. A.; and Golkar, E. (2018). An automated liver tumour segmentation from abdominal CT scans for hepatic surgical planning. *Int. J. Comput. Assist. Radiol. Surg.* 13, 1169–1176
- [2] Selle, D.; Preim, B.; Schenk, A.; and Peitgen, H. O. (2002). Analysis of vasculature for liver surgical planning. *IEEE Trans. Med. Imaging* 21, 1344–1357
- [3] Sanchez-Castro, F.-J.; Thierry, L.; Mory, B.; and Ardon, R. (2010). Automatic Inferior Vena Cava Segmentation for Hepatic Surgery Planning in Contrast-Enhanced CT Images. *Comput. Assist. Radiol. Surgery*, 24th Int. Congr. Exhib. 5.
- [4] Alirr, O. I.; and Rahni, A. A. A. (2016). Development of automatic segmentation of the inferior vena cava in abdominal CT scans. in 2016 IEEE EMBS Conference on Biomedical Engineering and Sciences (IECBES) 235–239
- [5] Alirr, O. I.; and Rahni, A. A. A. (2019). Survey on Liver Tumour Resection Planning System: Steps, Techniques, and Parameters. *J. Digit. Imaging* 1–20
- [6] Pamulapati, V.; Wood, B. J.; and Linguraru, M. G. (2011). Intra-hepatic vessel segmentation and classification in multi-phase CT using optimized graph cuts. in *Biomedical Imaging: From Nano to Macro*, 2011 IEEE International Symposium on 1982–1985
- [7] Chi, Y.; Liu, J.; and Venkatesh, SK. (2011). Segmentation of liver vasculature from contrast enhanced CT images using context-based voting. *IEEE Trans. Biomed. Eng.* 58, 2144–2153 (2011)
- [8] Conversano, F.; Franchini, R.; and Demitri, C. (2011). Hepatic Vessel Segmentation for 3D Planning of Liver Surgery. Experimental Evaluation of a New Fully Automatic Algorithm. *Acad. Radiol.* 18, 461–470 (2011)
- [9] Kim, D. (2013). Hepatic vessel segmentation on contrast enhanced CT image sequence for liver transplantation planning. *J. Biomed. Sci. Eng.* 06, 498–503
- [10] Jin, J.; Yang, L.; Zhang, X. and Ding, M. (2013). Vascular tree segmentation in medical images using Hessianbased multiscale filtering and level set method. *Comput. Math. Methods Med.* 2013, 1–10
- [11] Yureidini, A.; Kerrien, E.; Loria, I. N. G. and Nord-europe, I. L. (2012). Robust RANSAC-based blood vessel segmentation. *Proc. SPIE* 8314, 8314M
- [12] Beichel, R.; Pock, T.; and Janko, C. (2004). Liver segment approximation in CT data for surgical resection planning. *Proc. SPIE* 5370, 1435–1446
- [13] Marcan, M.; Pavliha, D.; and Music, MM. (2014). Segmentation of hepatic vessels from MRI images for planning of electroporation-based treatments in the liver. *Radiol. Oncol.* 48, 267–81
- [14] Esneault, S.; Lafon, C. and Dillenseger, J.-L. (2010) Liver Vessels Segmentation Using a Hybrid Geometrical Moments/Graph Cuts Method. *IEEE Trans. Biomed. Eng.* 57, 276–283
- [15] Lesage, D.; Angelini, E. D.; Bloch, I. and Funka-Lea, G. (2009). A review of 3D vessel lumen segmentation techniques: Models, features and extraction schemes. *Med. Image Anal.* 13, 819–845
- [16] Mohan, V.; Sundaramoorthi, G.; Stillman, A. and Tannenbaum, A. (2009). Vessel Segmentation with Automatic Centerline Extraction Using Tubular Tree Segmentation. 8 pages
- [17] Shen, Y.; Wang, B.; Ju, Y. and Xie, J. (2006). Interaction techniques for the exploration of hepatic vessel structure. *Eng. Med*
- [18] Soler, L.; Delingette, H.; and Malandain, G. (2001). Fully automatic anatomical, pathological, and functional segmentation from CT scans for hepatic surgery. *Comput. Aided Surg.* 6, 131–142
- [19] Smistad, E.; Elster, A. C.; and Lindseth, F. (2014). GPU accelerated segmentation and centerline extraction of tubular structures from medical images. *Int. J. Comput. Assist. Radiol. Surg.* 9, 561–575
- [20] Rodrigues, F. M.; Silva, J. S.; and Rodrigues, T. M. (2012). An algorithm for the surgical planning of hepatic resections. 2012 IEEE 2nd Port. Meet. Bioeng. ENBENG 2012
- [21] Oliveira, D. A.; Feitosa, R. Q.; and Correia, M. M. (2011). Segmentation of liver, its vessels and lesions from CT images for surgical planning. *Biomed. Eng. Online* 10, 30
- [22] Zeng, Y. Z., Liao, S. H., Tang, P., Zhao, Y. Q., Liao, M., Chen, Y., and Liang, Y. X. (2018). Automatic liver vessel segmentation using 3D region growing and hybrid active contour model. *Computers in biology and medicine*, 97: 63-73
- [23] Luu, H. M.; Klink, C.; Moelker, A.; Niessen, W. and van Walsum, T. (2015). Quantitative evaluation of noise reduction and vesselness filters for liver vessel segmentation on abdominal CTA images. *Phys. Med. Biol.* 60, 3905–26
- [24] Tian, Y.; Chen, Q.; and Wang, W. (2014). A vessel active contour model for vascular segmentation. *Biomed Res. Int.* 2014
- [25] Hong, Q.; Li, Q.; and Wang, B. (2014). 3D vasculature segmentation using localized hybrid level-set method. *Biomed. Eng. Online* 13, 169
- [26] Kaftan, J. N.; Tek, H. and Aach, T. (2009). A two-stage approach for fully automatic segmentation of venous vascular structures in liver CT images. *Proc. SPIE* 725911-725911–12
- [27] Zhan, Y.; Qian, Y.; and Liao, M. (2016). Liver vessel segmentation based on extreme learning machine. *Phys. Medica* 32, 709–716

- [28] Alirr, O. I.; and Rahni, A. A. A. (2018). Automatic liver segmentation from CT scans using intensity analysis and level-set active contours. *J. Eng. Sci. Technol.*, 13(11), 3821-3839
- [29] Frangi, A. F.; Niessen, W. J.; Vincken, K. L. and Viergever, M. (1998). Multiscale vessel enhancement filtering. *Medial Image Comput. Comput. Invervention - MICCAI'98. Lect. Notes Comput. Sci.* vol 1496 1496, 130–137.
- [30] Mendrik, A. M.; Vonken, E. J.; Rutten, A.; Viergever, M. A. and Van Ginneken, B. (2009). Noise reduction in computed tomography scans using 3-D anisotropic hybrid diffusion with continuous switch. *IEEE Trans. Med. Imaging* 28, 1585–1594
- [31] Weickert, J. (1998). Anisotropic diffusion in image processing. *Image Rochester NY* 256, 170
- [32] Selle, D.; Preim, B.; Schenk, A. and Peitgen, H.-O. (2002). Analysis of vasculature for liver surgical planning. *IEEE Trans. Med. Imaging* 21, 1344–1357
- [33] Smistad, E.; Elster, A. C. and Lindseth, F. (2014). GPU accelerated segmentation and centerline extraction of tubular structures from medical images. *Int. J. Comput. Assist. Radiol. Surg.* 9, 561–575
- [34] Zhang, R., Zhou, Z., Wu, W., Lin, C. C., Tsui, P. H., and Wu, S. (2018). An improved fuzzy connectedness method for automatic three-dimensional liver vessel segmentation in CT images. *Journal of Healthcare Engineering*, 2018
- [35] Zhang, H., Bai, P., Min, X., Liu, Q., Ren, Y., Li, H., and Li, Y. (2020). Hepatic vessel segmentation based on an improved 3D region growing algorithm. In *Journal of Physics: Conference Series*, 1486: 032038